ISSN 0021-3640, JETP Letters, 2026, Vol. 123, No. 4, pp. 265–270. © The Author(s), 2026. This article is an open access publication.
Russian Text © The Author(s), 2026, published in Pis'ma v Zhurnal Eksperimental'noi i Teoreticheskoi Fiziki, 2026, Vol. 123, No. 4, pp. 286–292.

CONDENSED MATTER

Subdomain Structure in a Single Crystal of the Magnetic Topological Insulator $MnSb_2Te_4$

V. A. Tyutvinov[a,b,*], M. S. Sidelnikov[a], N. A. Abdullayev[c,d], Z. S. Aliev[c,d], I. R. Amiraslanov[c,d], N. T. Mamedov[c,d], V. N. Zverev[a], and L. Ya. Vinnikov[a]

[a] *Osipyan Institute of Solid State Physics, Russian Academy of Sciences, Chernogolovka, Moscow region, 142432 Russia*
[b] *Moscow Institute of Physics and Technology (National Research University), Dolgoprudny, Moscow region, 141700 Russia*
[c] *Institute of Physics, Ministry of Science and Education, AZ 1073 Baku, Azerbaijann*
[d] *Baku State University, AZ 1148 Baku, Azerbaijan*
**e-mail: tiutvinov.va@phystech.edu*

Received November 20, 2025; revised December 27, 2025; accepted January 12, 2026

The domain structure of a $MnSb_2Te_4$ single crystal with a Curie temperature of $T_C \approx 45$ K has been studied using the high-resolution Bitter decoration technique. Magnetotransport measurements have confirmed soft ferromagnetic ordering with a coercive field of about 100 Oe. The formation of a hierarchical domain structure characterized by two distinct spatial scales has been revealed. These results indicate the existence of weakly magnetically coupled surface and bulk subsystems. The observed subdomain structure can be attributed to the formation of a ferromagnetic barrier due to an inhomogeneous distribution of Mn_{Sb} antisite defects with an additional contribution from symmetry breaking in the near-surface layer.

DOI: 10.1134/S002136402561019X

1. INTRODUCTION

The discovery of intrinsic magnetic topological insulators, such as $MnBi_2Te_4$, has stimulated intensive research on the quantum anomalous Hall effect (QAHE) [1–5], the axion insulator state [6], and Weyl semimetals [7]. The prospect of realizing the QAHE in the $MnBi_2Te_4$ system without an external magnetic field opens up opportunities for creating energy-efficient spintronic devices. However, practical implementations are hindered by fundamental limitations: high bulk *n*-type conductivity in $MnBi_2Te_4$ [8], which complicates the observation of chiral edge states [9], and a low magnetic ordering temperature not exceeding 26 K [1, 10].

One of the approaches to suppress the bulk conductivity is the isovalent substitution of antimony for bismuth, leading to the formation of $MnSb_2Te_4$. $MnSb_2Te_4$ crystals are structural analogs of $MnBi_2Te_4$ [11–13]. This structural similarity is confirmed by X-ray diffraction studies, as well as by investigations of $MnBi_{0.5}Sb_{1.5}Te_4$ solid solutions [14].

The magnetic ground state of stoichiometric $MnSb_2Te_4$ has an A-type antiferromagnetic order [15, 16]. However, antisite defects, in particular Mn_{Sb}, make decisive contribution to the magnetic properties of $MnSb_2Te_4$ and induce ferromagnetic ordering [17, 18]. Moreover, controlled manganese enrichment and the concomitant increase in the concentration of antisite defects can increase the Curie temperature T_C up to 45–50 K [19], thereby opening a route toward the realization of the QAHE at temperatures well above liquid helium temperatures.

Previous magnetic force microscopy studies of the magnetic structure of $MnSb_2Te_4$ have focused on domain walls in the antiferromagnetic phase [20], the direct visualization of ferromagnetism in samples with $T_C \approx 33$ K [21], and the control of stripe and bubble domains in ferrimagnetic films with $T_C \approx 27$ K [22]. However, the nature of the domain structure in bulk $MnSb_2Te_4$ single crystals with a high Curie temperature T_C is still unclear, as an increased concentration of antisite defects may give rise to pronounced magnetic inhomogeneity. Furthermore, alternative magnetic imaging techniques, such as the Bitter decoration technique [23], which eliminates the influence of a magnetic probe on the domain structure, have not yet been employed to study these systems.

In this work, we investigate the domain structure of a $MnSb_2Te_4$ single crystal with a Curie temperature of $T_C \approx 45$ K, using the high-resolution Bitter decoration technique with magnetic nanoparticles. The domain structure characterized by two distinct spatial scales is observed. The results are discussed in the context of an inhomogeneous distribution of Mn_{Sb} antisite defects with a possible additional contribution from inversion symmetry breaking in the near-surface layer.

2. METHODS

The $MnSb_2Te_4$ single crystal was obtained by cleaving from an ingot grown by the directional crystallization method [11]. The sample had the form of a thin plate with dimensions of ~3.5 × 3.5 × 0.16 mm and was characterized by X-ray diffraction and Raman scattering at room temperature [12].

Electrical contacts for transport measurements were fabricated using conductive graphite paste. The measurements were performed in a liquid-helium cryostat equipped with a superconducting solenoid. The external magnetic field was applied along the crystallographic **c** axis, which is perpendicular to the basal plane of the sample. The electrical resistance and Hall effect were measured in a standard four-probe geometry using an ac lock-in technique at a frequency of 20 Hz.

Prior to the decoration experiments, the surface of the single crystal was prepared by mechanical exfoliation using adhesive tape to remove surface contamination and oxide layers.

To visualize the domain structure in a bulk $MnSb_2Te_4$ single crystal, the high-resolution Bitter decoration technique with iron magnetic nanoparticles was employed [23]. The experiments were carried out using a cryogenic insert without active sample temperature control. Compared to magnetic force microscopy, this technique has two key advantages: it is less sensitive to surface quality and eliminates artifacts associated with the direct influence of a magnetic probe on the domain structure.

The initial helium pressure and temperature in the decoration chamber were ~0.07 Torr and 4.3 K, respectively. The nanoparticle deposition process was initiated by a rectangular current pulse with an amplitude of 12 A and a duration of (2.2 ± 0.3) s applied to the evaporator. During deposition, the pressure in the chamber was increased to 0.11 Torr and the temperature reached ~6 K.

A 240-nm-thick niobium (Nb) film with a superconducting transition temperature $T_{sc} \approx 9$ K was used as a reference sample.

The samples were cooled to the experimental working temperature in zero external magnetic field ($B_{ext} \approx 0$, zero-field cooling). After thermal equilibrium was established at $T \approx 4.3$ K, the single crystal was exposed to a magnetic field of 50 Oe perpendicular to its basal plane. The magnetic field was generated by a solenoid with a copper winding.

3. RESULTS AND DISCUSSION

The investigated $MnSb_2Te_4$ single crystal exhibits ferromagnetic behavior. Figure 1 shows the results of magnetotransport measurements. The temperature dependence of the resistivity $\rho(T)$ [24] has a maximum

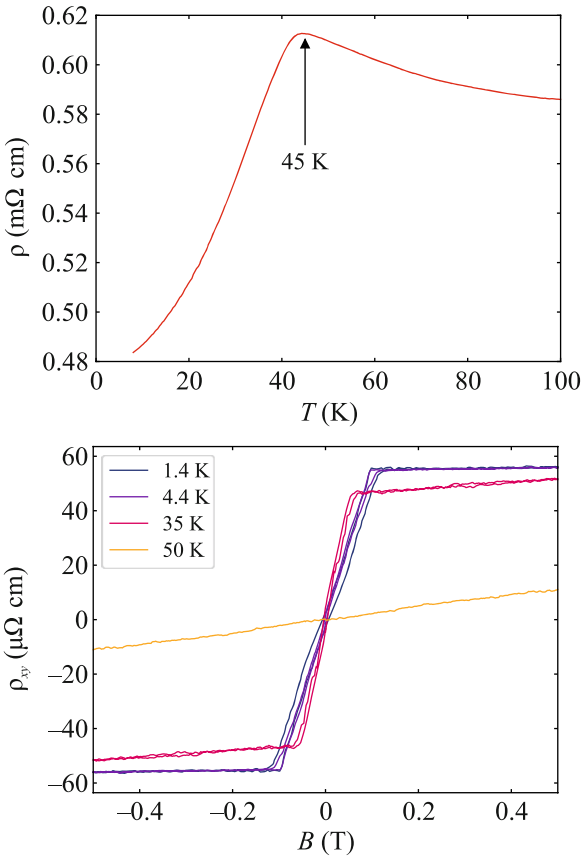


Fig. 1. (Color online) (Top panel) Temperature dependence of the resistivity $\rho(T)$ of the $MnSb_2Te_4$ single crystal measured in zero magnetic field. (Bottom panel) Transverse (Hall) resistivity $\rho_{xy}(B)$ of the $MnSb_2Te_4$ single crystal measured at different temperatures versus the perpendicular magnetic field B.

near $T_C \approx 45$ K, which corresponds to the paramagnetic to ferromagnetic phase transition.

The presence of spontaneous magnetization in the ferromagnetic phase is confirmed by the observation of the Hall resistivity ρ_{xy} (see Fig. 1). The dependences $\rho_{xy}(B)$ exhibit a hysteretic behavior with a low coercive field $H_c \sim 100$ Oe, which is characteristic of soft magnetic materials.

The morphology of the domain structure was investigated using the high-resolution Bitter decoration technique. In the reference Nb film sample, zero-field cooling revealed a dendritic magnetic flux penetration pattern typical of type-II superconductors [25].

Figure 2 presents the results of magnetic flux visualization in different regions of the $MnSb_2Te_4$ single crystal with a thickness of (160 ± 20) μm. In surface regions 1–4, two-scale domain structures are observed, while the majority of the surface exhibits a typical stripe domain pattern with isolated bubble inclusions, which is characteristic of ferromagnets

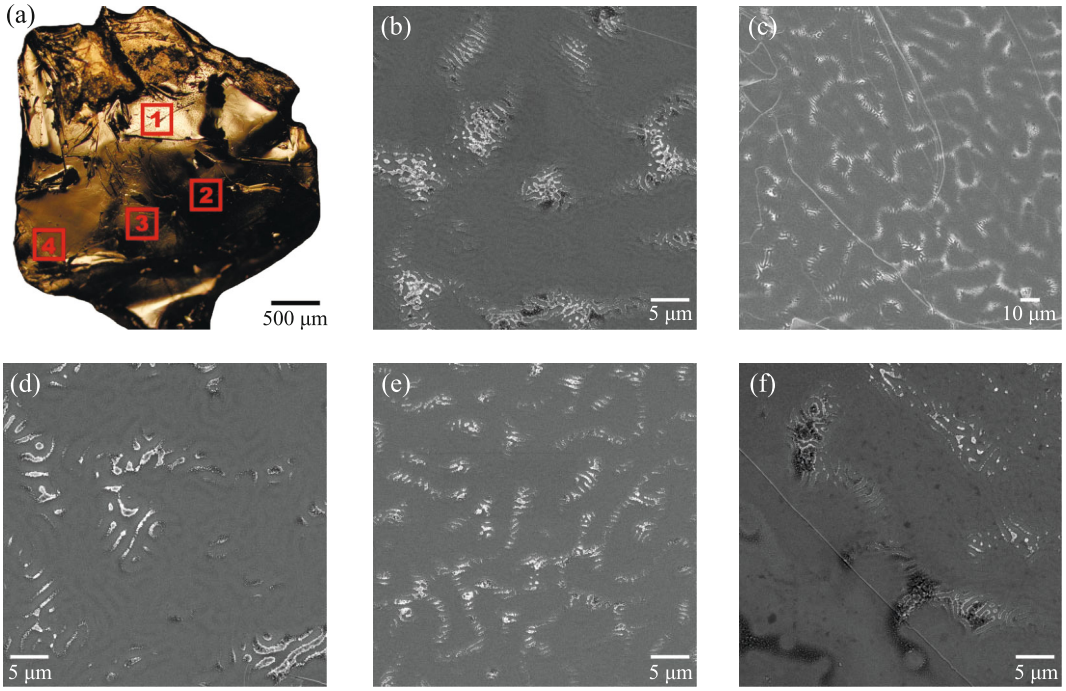


Fig. 2. (Color online) Micrographs of the surface and decoration patterns of the $MnSb_2Te_4$ single crystal. (a) Optical microscopy image of the crystal surface. (b–f) Scanning electron microscopy images of the magnetic flux structure in (b) region 1, (c) region 2, (d, e) region 3, and (f) region 4 of the sample indicated in panel (a) and obtained by decoration with magnetic nanoparticles.

with a strong uniaxial anisotropy [26]. The two-scale domain structure is spatially localized and covers less than 10% of the investigated surface. However, it is reproducible in repeated experiments after exfoliation of the surface layer (typically about 10 μm), indicating the robustness of the observed effect.

The observed decoration patterns reflect the magnetic flux distribution above the sample surface, which is confirmed by several independent experimental observations. In particular, domain stripes continuously cross natural crystal surface steps with height variations of tens of nanometers (see Fig. 2c), and qualitatively similar decoration patterns are reproducibly obtained in independent experiments carried out under identical conditions.

The contrast in decoration images is governed by the spatial distribution of the stray magnetic field above the sample surface. Iron nanoparticles, being in a superparamagnetic or ferromagnetic state, become magnetized by the external magnetic field and are preferentially deposited in regions with the maximum normal component of the stray field [27]. As a result, the local particle density is proportional to the magnetic flux density, providing a direct correspondence between the decoration pattern and the domain structure.

Differences in contrast between optical microscopy and scanning electron microscopy images acquired by arise from the distinct image-formation mechanisms of these techniques. Regions with a high density of deposited particles appear dark in optical microscopy images, whereas they are brighter in scanning electron microscopy images.

The observed features of the domain structure exhibit signatures of self-similarity: large-scale domains with a characteristic period on the order of tens of micrometers contain embedded subdomain patterns.

For a quantitative characterization of the domain structure, Fourier analysis of the optical images was performed (see Fig. 3). The resulting spatial spectra reveal distinct characteristic frequencies corresponding to two spatial scales of the magnetic texture.

After the binarization of the images (see Figs. 3a and 3b), the average periods of the domain structure were determined to be $\lambda_1 = 14.2$ μm, $\Delta\lambda_1 = 1.1$ μm, and $\lambda_2 = 1.82$ μm, and $\Delta\lambda_2 = 0.24$ μm for the large- and small-scale components, respectively. The ratio of the characteristic periods is approximately 7.8, indicating the formation of a hierarchical domain structure with two clearly separated spatial scales.

The comparison of optical microscopy and scanning electron microscopy images (see Fig. 3) demonstrates good agreement in the overall domain morphology. Minor differences in the apparent domain width can be attributed to optical diffraction broadening.

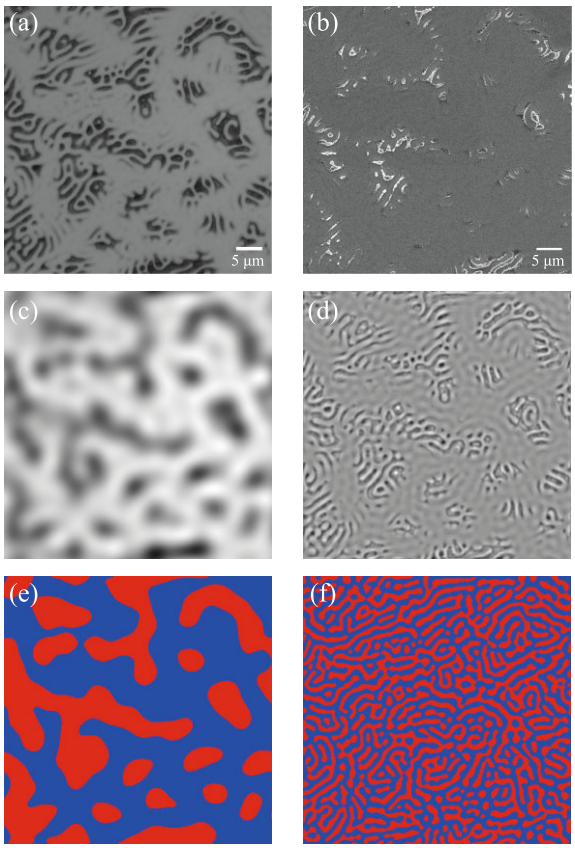


Fig. 3. (Color online) Comparative analysis of the domain structure in $MnSb_2Te_4$. (a) Optical and (b) scanning electron microscopy images of domain morphology obtained after decoration with magnetic nanoparticles. (c) Small- and (d) large-scale components of the domain structure separated due to the spatial frequency analysis. (e, f) Binarized images corresponding to the (e) large- and (f) small-scale domain structures.

The observed Curie temperature $T_C \approx 45$ K is in good agreement with the data reported in [19], where similar temperatures were achieved in Mn-enriched $MnSb_2Te_4$ samples. This consistency confirms that the controlled introduction of Mn_{Sb} antisite defects provides an efficient route to increase the Curie temperature in this class of materials.

Indirect signs of the stratification of magnetic subsystems were previously detected in features of the anomalous Hall effect in doped vanadium crystals [28]. However, direct visualization of a subdomain structure has so far been achieved only in the van der Waals magnet $CrBr_3$ using magnetic force microscopy [29], where the effect was relatively weak, likely due to the limited sensitivity of the technique. In this work, optical microscopy after decoration enables clear identification of the two-scale domain structure.

The physical origin of magnetic stratification remains unclear. In $CrBr_3$, it is attributed to the formation of a magnetic barrier at stacking faults, a concept that was generalized to all van der Waals crystals [29]. However, for compounds of the $Mn(Sb, Bi)_2Te_4$ family, experimental evidence for such stacking faults is lacking [17, 18].

We assume that the observed separation of magnetic subsystems into surface and bulk components may be due to the formation of a magnetic barrier, analogous stacking fault discussed for $CrBr_3$ [29]. In the case of $MnSb_2Te_4$, such a barrier is likely governed by a different microscopic mechanism and can originate from an inhomogeneous distribution of Mn_{Sb} antisite defects. An additional contribution may come from symmetry reduction in the near-surface layer, resulting from inversion symmetry breaking and the formation of point defects during exfoliation [30, 31]. These effects can modify exchange and dipole interactions, as well as magnetic anisotropy [32].

As a result, two weakly magnetically coupled subsystems with different effective magnetic layer thicknesses are formed. The observed self-similarity of the domain structure across both spatial scales is consistent with the fact that domain morphology is governed by the balance of exchange, dipole, and magnetostatic interactions and magnetic anisotropy. These interactions are qualitatively similar in the bulk and near the surface, but scale quantitatively with the effective layer thickness. Consequently, the revealed subdomain morphology (see Fig. 3) can be interpreted as a superposition of two self-similar domain structures formed in weakly coupled surface and bulk magnetic layers. The precise microscopic mechanism of such stratification requires further experimental and theoretical investigation.

4. CONCLUSIONS

In this work, a subdomain magnetic structure characterized by two distinct spatial scales has been discovered in a $MnSb_2Te_4$ single crystal with a Curie temperature of ~45 K using the high-resolution Bitter decoration technique. The observed qualitative difference in domain morphology compared to previously studied samples with lower Curie temperatures suggests a possible relation between the ferromagnetic ordering temperature and the characteristics of the domain structure.

The two-scale domain structure has been attributed to the superposition of two weakly magnetically coupled subsystems with different effective magnetic layer thicknesses and characteristic domain sizes. The formation of a magnetic barrier associated with an inhomogeneous distribution of Mn_{Sb} antisite defects, with an additional contribution from inversion symmetry breaking in the near-surface layer has been discussed as a possible mechanism. It should be emphasized that this interpretation is qualitative and requires further experimental and theoretical verification.

A promising direction for future research is a systematic investigation of the domain structure across a series of samples with different Curie temperatures, which would enable testing a possible correlation between magnetic order parameters and domain morphology. Micromagnetic modeling aimed at elucidating the role of defects and surface effects in van der Waals magnetic topological materials could provide further insight into the mechanisms responsible for the observed structure.

ACKNOWLEDGMENTS

We are grateful to S.V. Egorov and A.S. Astrakhantseva for conducting the SEM studies and to the team of the Laboratory of Superconductivity at the Institute of Solid State Physics, Russian Academy of Sciences, in particular, to V.V. Ryazanov, N.A. Tulina, and A.S. Ionin for fruitful discussions.

FUNDING

This work was supported by the ongoing funding of the Osipyan Institute of Solid State Physics, Russian Academy of Sciences and the Institute of Physics, Ministry of Science and Education of Azerbaijan. No additional grants to carry out or direct this particular research were obtained.

CONFLICT OF INTEREST

The authors of this work declare that they have no conflicts of interest.

OPEN ACCESS

This article is licensed under a Creative Commons Attribution 4.0 International License, which permits use, sharing, adaptation, distribution and reproduction in any medium or format, as long as you give appropriate credit to the original author(s) and the source, provide a link to the Creative Commons license, and indicate if changes were made. The images or other third party material in this article are included in the article's Creative Commons license, unless indicated otherwise in a credit line to the material. If material is not included in the article's Creative Commons license and your intended use is not permitted by statutory regulation or exceeds the permitted use, you will need to obtain permission directly from the copyright holder. To view a copy of this license, visit http://creativecommons.org/licenses/by/4.0/

REFERENCES

1. M. M. Otrokov, I. I. Klimovskikh, H. Bentmann, et al., "Prediction and observation of an antiferromagnetic topological insulator," Nature (London, U.K.) **576**, 416 (2019).
2. Y. Deng, Y. Yu, M. Z. Shi, Z. Guo, Z. Xu, J. Wang, X. H. Chen, and Y. Zhang, "Quantum anomalous Hall effect in intrinsic magnetic topological insulator $MnBi_2Te_4$," Science (Washington, DC, U. S.) **367**, 895 (2020).
3. Y. Tokura, K. Yasuda, and A. Tsukazaki, "Magnetic topological insulators," Nat. Rev. Phys. **1**, 126 (2019).
4. B. A. Bernevig, C. Felser, and H. Beidenkopf, "Progress and prospects in magnetic topological materials," Nature (London, U.K.) **603**, 41 (2022).
5. A. Yu. Vyazovskaya, M. Bosnar, E. V. Chulkov, and M. M. Otrokov, "Intrinsic magnetic topological insulators of the $MnBi_2Te_4$ family," Commun. Mater. **6**, 88 (2025).
6. C. Liu, Y. Wang, H. Li, Y. Wu, Y. Li, J. Li, K. He, Y. Xu, J. Zhang, and Y. Wang, "Robust axion insulator and Chern insulator phases in a two-dimensional antiferromagnetic topological insulator," Nat. Mater. **19**, 522 (2020).
7. P. Li, J. Yu, Y. Wang, and W. Luo, "Electronic structure and topological phases of the magnetic layered materials $MnBi_2Te_4$, $MnBi_2Se_4$, and $MnSb_2Te_4$," Phys. Rev. B **103**, 155118 (2021).
8. B. Chen, F. Fei, D. Zhang, et al., "Intrinsic magnetic topological insulator phases in the Sb doped $MnBi_2Te_4$ bulks and thin flakes," Nat. Commun. **10**, 4469 (2019).
9. J. Zhu, Y. Feng, X. Zhou, et al., "Direct observation of chiral edge current at zero magnetic field in a magnetic topological insulator," Nat. Commun. **16**, 963 (2025).
10. A. Zeugner, F. Nietschke, A. U. B. Wolter, et al., "Chemical aspects of the candidate antiferromagnetic topological insulator $MnBi_2Te_4$," Chem. Mater. **31**, 2795 (2019).
11. Z. S. Aliev, I. R. Amiraslanov, D. I. Nasonova, A. V. Shevelkov, N. A. Abdullayev, Z. A. Jahangirli, E. N. Orujlu, M. M. Otrokov, N. T. Mamedov, M. B. Babanly, and E. V. Chulkov, "Novel ternary layered manganese bismuth tellurides of the $MnTe–Bi_2Te_3$ system: Synthesis and crystal structure," J. Alloys Compd. **789**, 443 (2019).
12. A. A. Maksimov, I. I. Tartakovskii, Z. S. Aliev, I. R. Amiraslanov, N. A. Abdullaev, V. N. Zverev, Z. A. Jahangirli, I. Yu. Sklyadneva, M. M. Otrokov, N. T. Mamedov, and E. V. Chulkov, "Temperature studies of Raman spectra in $MnBi_2Te_4$ and $MnSb_2Te_4$ magnetic topological insulators," JETP Lett. **118**, 357 (2023).
13. S. V. Eremeev, I. P. Rusinov, Yu. M. Koroteev, A. Yu. Vyazovskaya, M. Hoffmann, P. M. Echenique, A. Ernst, M. M. Otrokov, and E. V. Chulkov, "Topological magnetic materials of the $(MnSb_2Te_4)$ $(Sb_2Te_3)_n$ van der Waals compounds family," J. Phys. Chem. Lett. **12**, 4268 (2021).
14. N. A. Abdullayev, Kh. V. Aliguliyeva, V. N. Zverev, Z. S. Aliev, I. R. Amiraslanov, M. B. Babanly, Z. A. Jahangirli, Ye. N. Aliyeva, Kh. N. Akhmedova, T. G. Mammadov, M. M. Otrokov, A. M. Shikin, N. T. Mamedov, and E. V. Chulkov, "The charge transport mechanism in a new magnetic topological insulator $MnBi_{0.5}Sb_{1.5}Te_4$," Phys. Solid State **63**, 1120 (2021).
15. Z. Zang, Y. Zhu, M. Xi, et al., "Layer-number-dependent antiferromagnetic and ferromagnetic behavior in $MnSb_2Te_4$," Phys. Rev. Lett. **128**, 017201 (2022).

16. J.-Q. Yan, S. Okamoto, M. A. McGuire, A. F. May, R. J. McQueeney, and B. C. Sales, "Evolution of structural, magnetic, and transport properties in $MnBi_{2-x}Sb_xTe_4$," Phys. Rev. B **100**, 104409 (2019).

17. Y. Liu, L.-L. Wang, Q. Zheng, et al., "Site mixing for engineering magnetic topological insulators," Phys. Rev. X **11**, 021033 (2021).

18. C. Hu, S.-W. Lien, E. Feng, S. Mackey, H.-J. Tien, I. I. Mazin, H. Cao, T.-R. Chang, and N. Ni, "Tuning magnetism and band topology through antisite defects in Sb-doped $MnBi_4Te_7$," Phys. Rev. B **104**, 054422 (2021).

19. S. Wimmer, J. Sánchez-Barriga, P. Küppers, et al., "Mn-rich $MnSb_2Te_4$: A topological insulator with magnetic gap closing at high Curie temperatures of 45–50 K," Adv. Mater. **33**, 2102935 (2021).

20. P. M. Sass, W. Ge, J. Yan, D. Obeysekera, J. J. Yang, and W. Wu, "Magnetic imaging of domain walls in the antiferromagnetic topological insulator $MnBi_2Te_4$," Nano Lett. **20**, 2609 (2020).

21. W. Ge, P. M. Sass, J. Yan, S. H. Lee, Z. Mao, and W. Wu, "Direct evidence of ferromagnetism in $MnSb_2Te_4$," Phys. Rev. B **103**, 134403 (2021).

22. T. A. Webb, A. N. Tamanna, X. Ding, N. Verma, J. Xu, L. Krusin-Elbaum, C. R. Dean, D. N. Basov, and A. N. Pasupathy, "Tunable magnetic domains in ferrimagnetic $MnSb_2Te_4$," Nano Lett. **24**, 4393 (2024).

23. L. Ya. Vinnikov, I. S. Veshchunov, M. S. Sidelnikov, and V. S. Stolyarov, "The high-resolution Bitter decoration technique for the magnetic flux structure imaging at low temperatures," Instrum. Exp. Tech. **62**, 587 (2019).

24. V. N. Zverev, N. A. Abdullaev, Z. S. Aliev, I. R. Amiraslanov, Z. A. Dzhakhangirli, I. I. Klimovskikh, A. A. Ryabkina, A. M. Shikin, and N. T. Mamedov, "Low-temperature magnetotransport and magnetic properties of $MnSb_2Te_4$ crystals," Zh. Eksp. Teor. Fiz. **169**, 110 (2026).

25. C. A. Durán, P. L. Gammel, R. E. Miller, and D. J. Bishop, "Observation of magnetic-field penetration via dendritic growth in superconducting niobium films," Phys. Rev. B **52**, 75 (1995).

26. A. Hubert and R. Schäfer, *Magnetic Domains: The Analysis of Magnetic Microstructures* (Springer, Heidelberg, 1998), Chap. 3.7.3, p. 287.

27. T. Sakurai and Y. Shimada, "Application of the gas evaporation method to observation of magnetic domains," Jpn. J. Appl. Phys. **31**, 1905 (1992).

28. K. M. Fijalkowski, M. Hartl, M. Winnerlein, P. Mandal, S. Schreyeck, K. Brunner, C. Gould, and L. W. Molenkamp, "Coexistence of surface and bulk ferromagnetism mimics skyrmion Hall effect in a topological insulator," Phys. Rev. X **10**, 011012 (2020).

29. S. Y. Grebenchuk, M. Grzeszczyk, Z. Chen, M. Šiškins, V. Borisov, M. Pereiro, M. I. Katsnelson, O. Eriksson, K. S. Novoselov, and M. Koperski, "Correlations in magnetic sub-domains as an unconventional phase diagram for van der Waals ferromagnets," Adv. Sci. **12**, 2500562 (2025).

30. P. M. Sass, J. Kim, D. Vanderbilt, J. Yan, and W. Wu, "Robust A-type order and spin-flop transition on the surface of the antiferromagnetic topological insulator $MnBi_2Te_4$," Phys. Rev. Lett. **125**, 037201 (2020).

31. A. M. Shikin, D. A. Estyunin, I. I. Klimovskikh, et al., "Nature of the Dirac gap modulation and surface magnetic interaction in axion antiferromagnetic topological insulator $MnBi_2Te_4$," Sci. Rep. **10**, 13226 (2020).

32. I. P. Rusinov, V. N. Men'shov, and E. V. Chulkov, "Spectral features of magnetic domain walls on the surface of three-dimensional topological insulators," Phys. Rev. B **104**, 035411 (2021).

Translated by the authors

Publisher's Note. Pleiades Publishing remains neutral with regard to jurisdictional claims in published maps and institutional affiliations.

AI tools may have been used in the translation or editing of this article.